

Efficient Deep Reinforcement Learning with Imitative Expert Priors for Autonomous Driving

Zhiyu Huang, *Student Member, IEEE*, Jingda Wu, *Student Member, IEEE*, Chen Lv, *Senior Member, IEEE*

Abstract—Deep reinforcement learning (DRL) is a promising way to achieve human-like autonomous driving. However, the low sample efficiency and difficulty of designing reward functions for DRL would hinder its applications in practice. In light of this, this paper proposes a novel framework to incorporate human prior knowledge in DRL, in order to improve the sample efficiency and save the effort of designing sophisticated reward functions. Our framework consists of three ingredients, namely expert demonstration, policy derivation, and reinforcement learning. In the expert demonstration step, a human expert demonstrates their execution of the task, and their behaviors are stored as state-action pairs. In the policy derivation step, the imitative expert policy is derived using behavioral cloning and uncertainty estimation relying on the demonstration data. In the reinforcement learning step, the imitative expert policy is utilized to guide the learning of the DRL agent by regularizing the KL divergence between the DRL agent’s policy and the imitative expert policy. To validate the proposed method in autonomous driving applications, two simulated urban driving scenarios (unprotected left turn and roundabout) are designed. The strengths of our proposed method are manifested by the training results as our method can not only achieve the best performance but also significantly improve the sample efficiency in comparison with the baseline algorithms (particularly 60% improvement compared to soft actor-critic). In testing conditions, the agent trained by our method obtains the highest success rate and shows diverse driving behaviors as demonstrated by the human expert. We also demonstrate that the imitative expert policy with deep ensemble-based uncertainty estimation can lead to better performance, especially in a more difficult task. As a result, the proposed method has shown its potential to facilitate the applications of DRL-enabled human-like autonomous driving systems in practice.

Index Terms—Deep reinforcement learning, autonomous driving, imitative expert policy, uncertainty estimation.

I. INTRODUCTION

REINFORCEMENT learning (RL) has seen successful applications in a number of domains including autonomous driving [1] and intelligent transportation systems [2]. Using an RL-based decision-making system can deliver a human-like driving experience (featuring interaction awareness and personalization), by learning to interact with other agents on the road without explicitly modeling the environment and tweaking the reward functions to fit the preferences of different people. On the contrary, these are two problems that RL needs

to solve. One major problem of RL is the notoriously low data efficiency, which means an RL agent requires a massive amount of interactions with the environment to solve a problem. It even gets worse as we attempt to tackle increasingly demanding and diverse problems in autonomous driving, such as crossing an intersection or doing an unprotected left turn in dense traffic. Another challenge is the design of the reward function, which specifies the preference of behavior for the RL agent. A poorly designed reward function may cause the agent to mistakenly exploit the reward function and stick to unexpected behaviors, and thus it often takes a significant amount of time and effort to design a proper reward function. Although the reward function can be learned from human driving data [3], [4], some structure of the reward function (e.g., a linear combination of different hand-crafted features) is usually assumed, which might not stand in practice.

Facing these two major challenges, this paper proposes a novel RL framework that can transfer human prior knowledge into the RL agent with a small amount of human demonstration, in order to improve the sample efficiency and save the effort to design sophisticated reward functions. First of all, we distill the human prior knowledge through their demonstrations into the form of imitative expert policy using imitation learning and uncertainty estimation. Subsequently, the imitative expert policy is used to guide the learning process of RL agents through regularizing the RL policy to be close to the expert policy. The RL agent’s exploration ability is still maintained if the uncertainty of the imitative expert policy is high. We also demonstrate that human-like behaviors (driving preferences) are achievable with only a sparse reward function indicating whether the task succeeds. In detail, as shown in Fig. 1, we first obtain a stochastic expert policy using imitation learning from expert demonstration. By adding the Kullback–Leibler (KL) divergence between the imitative expert priors and agent policy into the RL framework, we can regularize the agent’s behaviors within the desired space, and thus the learning efficiency can be significantly enhanced. The main contributions of this paper are listed as follows.

- 1) An RL framework that incorporates the imitative expert priors from expert demonstrations is proposed. The imitative expert priors are learned with imitation learning and uncertainty quantification method, which can regularize the RL agent’s behavior while also maintaining its exploration ability.
- 2) Two different ways, namely policy penalty and policy constraint, are proposed to integrate the imitative expert policy in the framework of the actor-critic algorithm and

Z. Huang, J. Wu and C. Lv are with the School of Mechanical and Aerospace Engineering, Nanyang Technological University, Singapore, 639798. (e-mail: {zhiyu001,jingda001}@e.ntu.edu.sg, lyuchen@ntu.edu.sg)

Corresponding author: C. Lv.

This work was supported in part by A*STAR Grant (No. 1922500046), Singapore, the Alibaba Group through Alibaba Innovative Research (AIR) Program and Alibaba-NTU Singapore Joint Research Institute (JRI) (No. AN-GC-2020-012), and the SUG-NAP Grant, Nanyang Technological University, Singapore.

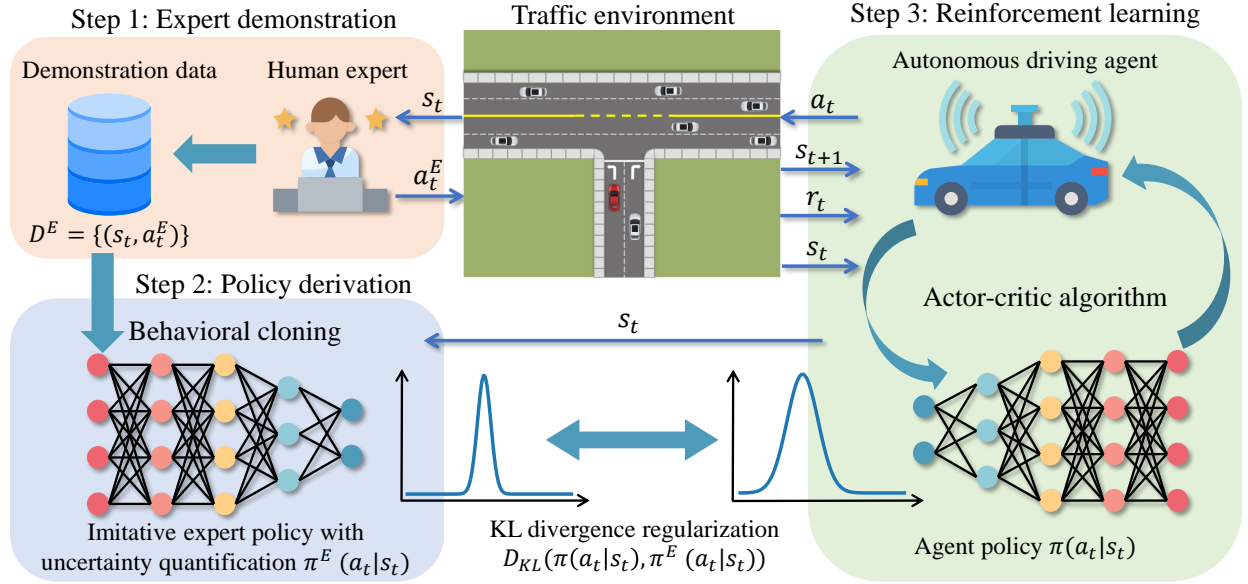


Fig. 1: The conceptual framework of our deep reinforcement learning method with imitative expert priors

their performances are investigated.

- 3) The proposed method is intensively tested in challenging urban driving scenarios and we demonstrate human-like driving behaviors emerge even the agent only gets sparse reward feedback from the environment. The effects of expert policies trained with different methods are also investigated.

II. RELATED WORK

A. Imitation learning and reinforcement learning

Imitation learning (IL) and reinforcement learning (RL) are two promising tools to be applied in autonomous driving, which can help develop an adaptive, flexible, and human-like decision-making or control system. Imitation learning, which employs an efficient supervised learning mechanism, has seen widespread use in autonomous driving research due to its simplicity and effectiveness. For example, imitation learning has been used in end-to-end autonomous driving systems that directly output control signals from raw sensor inputs [5], [6] or modular driving systems that output trajectories from processed perception information [7]. However, one intractable drawback of imitation learning is the distribution shift, which means compounding errors leads to system failure due to the mismatch of training and inference distributions. On the other hand, RL will not encounter this problem because it relies on online interactions with the environment, and thus RL is a better fit in autonomous driving research. Many works have utilized RL to tackle difficult tasks in autonomous driving, such as urban driving [8], multi-agent interactions [9], and handling near-accident scenarios [10]. However, the drawbacks of RL are obvious and unsolved, which could influence its applications in practical use. For one thing, the training of RL is very inefficient, even in the simulated environment, and for another, the reward function is difficult to specify and tuning of the parameters is time-consuming.

B. Learning with human prior knowledge

To improve the sample efficiency of RL or to inject some desired properties (e.g., safety, smoothness, and risk-averse in driving) into the RL policy, many works propose to incorporate human prior knowledge into the RL framework. Human prior knowledge can be their understanding of the task or their guidance and demonstration provided to the RL agent. Leveraging human understanding to the driving task can help solve it safely and efficiently. For example, [11], [12] proposed to add a safety check module encoding the expert-defined safety rules in the RL-based control system, to guide the exploration process and exclude dangerous actions, in order to prevent unsafe exploration and speed up training. [13] relied on learning useful skills first (driving-in-lane, left lane change, and right lane change) and then a master policy to switch between different skills, to hierarchically and efficiently solve the driving task. In addition, utilizing human guidance or demonstration helps constrain the solution space and guide the RL agent's exploration, to eliminate unwanted interactions and accelerate the learning process. For example, [14] proposed a real-time human-guidance-based learning method that lets human experts intervene in the training process in real-time and provide guidance and thereby enables the RL agent to learn from both human guidance and self-exploration, to boost the learning efficiency. However, this kind of method is heavily dependent on online human guidance, which may impose a heavy workload on human experts. On the other hand, the offline human demonstration is easy to obtain and does not require interactions between the RL agent and the human expert. However, how to incorporate human demonstration in the RL framework remains open.

C. Reinforcement learning with demonstrations

To make use of human demonstrations in RL, one approach is to pre-train the policy with imitation (supervised) learning

using the expert demonstrations to initialize the policy with a reasonable level of performance, and then apply RL to obtain a better policy with respect to the reward function [15], [16]. Nonetheless, this method often does not work well, especially for the maximum entropy RL [17] that encourages randomness of the policy to explore at the beginning. An alternate approach is to add the expert demonstrations into the experience replay buffer for off-policy RL algorithms and sample the experience from both expert demonstrations and agent's interactions to update the policy [18], [19]. However, this kind of approach requires annotating reward for each state-action pair to comply with the format of transition tuples in RL, which is intractable in some cases due to the inaccessibility of the expert reward. [14], [20] proposed to add imitation learning (minimizing the discrepancy between the agent actions and expert actions) to the policy update in addition to reinforcement learning (maximizing the Q values), to learn from both human demonstration and agent's self-exploration. However, a sophisticated design of reward function or reward shaping is still indispensable for these methods. On the other hand, our proposed method is inspired by the recent advances in offline RL [21], which is to constrain the agent policy and expert policy within a small deviation. This idea is originally brought forward to avoid value overestimation for actions outside of the training distribution, since the agent learns purely offline without online data collections. We propose to use such a method in an online RL setting where the expert policy is learned from expert demonstrations and then used to guide the exploration and constrain the RL agent's behaviors. To maintain the RL agent's exploration capability, we propose to use uncertainty estimation in deriving the expert policy with imitation learning, so that the agent is able to explore more when the uncertainty of the expert policy is high, meaning the action given by the imitative expert policy is not reliable. Moreover, the reward function design can be significantly simplified since the agent's behavior is regularized by the expert policy, thus allowing a sparse reward to use even in complicated situations.

III. BACKGROUND

A. Reinforcement learning

Reinforcement learning (RL) confronts the problem of learning to control a dynamic system, which can be fully defined by a Markov decision process (MDP), represented as $\mathcal{M} = (\mathcal{S}, \mathcal{A}, T, r, \gamma)$. In this tuple, \mathcal{S} is the state space $\mathbf{s} \in \mathcal{S}$, \mathcal{A} is the action space $\mathbf{a} \in \mathcal{A}$, T is the transition probability distribution that defines the system dynamics $T(\mathbf{s}_{t+1}|\mathbf{s}_t, \mathbf{a}_t)$, r is the reward function $r : \mathcal{S} \times \mathcal{A} \rightarrow \mathbb{R}$, and $\gamma \in (0, 1]$ is a discount factor. The target of RL is to acquire a policy, which is defined as a distribution over actions conditioned on states $\pi(\mathbf{a}_t|\mathbf{s}_t)$, in order to maximize the long-term discounted cumulative reward:

$$\max_{\pi} \mathbb{E}_{\tau \sim p_{\pi}(\tau)} \left[\sum_{t=0}^T \gamma^t r(\mathbf{s}_t, \mathbf{a}_t) \right], \quad (1)$$

where τ is a trajectory and $p_{\pi}(\tau)$ is the distribution of the trajectory under policy π , and T is the time horizon.

One way to optimize the target is to estimate the state or state-action value function, and then recover a policy. The state value function (V-function) and state-action value function (Q-function) are recursively defined as:

$$V^{\pi}(\mathbf{s}_t) = \mathbb{E}_{\mathbf{a}_t \sim \pi(\cdot|\mathbf{s}_t)} [Q^{\pi}(\mathbf{s}_t, \mathbf{a}_t)], \quad (2)$$

$$Q^{\pi}(\mathbf{s}_t, \mathbf{a}_t) = r(\mathbf{s}_t, \mathbf{a}_t) + \gamma \mathbb{E}_{\mathbf{s}_{t+1} \sim T(\cdot|\mathbf{s}_t, \mathbf{a}_t)} [V^{\pi}(\mathbf{s}_{t+1})]. \quad (3)$$

The optimal policy π^* can be obtained by maximizing $V^{\pi^*}(\mathbf{s})$ at all states $\mathbf{s} \in \mathcal{S}$. In the actor-critic method, which is illustrated in details in Section IV, one optimizes a policy π by alternating the learning of the V-function and Q-function through minimizing the Bellman errors over one-step transitions and learning of the policy through maximizing the Q-values.

In addition to maximizing the cumulative discounted reward, soft actor-critic (SAC) [17], [22] adds a maximum entropy term \mathcal{H} to the target so as to facilitate exploration, given by

$$\max_{\pi} \mathbb{E}_{\tau \sim p_{\pi}(\tau)} \left[\sum_{t=0}^T \gamma^t (r(\mathbf{s}_t, \mathbf{a}_t) + \alpha \mathcal{H}(\pi(\cdot|\mathbf{s}_t))) \right]. \quad (4)$$

The entropy term is equivalent to the KL divergence between the agent's policy and a uniformly random action prior. However, in our method, we regularize the learned policy π towards the non-uniform and informative expert behavior policy π^E . In addition to that, another way is proposed, which is to directly constrain the discrepancy between the learned policy π and the expert behavior policy π^E . Some methods of obtaining the expert policy π^E from demonstration data are described below.

B. Behavioral cloning

Since the expert policy is not directly accessible, one feasible and widely-used approach is to approximate the expert policy through imitation learning from expert demonstrations. Formally, given the expert demonstration dataset $\mathcal{D}^E : \{\tau_i\}_N$, which consists of N trajectories, and each trajectory is a sequence of state-action pairs $\tau = \{\mathbf{s}_1, \mathbf{a}_1, \dots, \mathbf{s}_T, \mathbf{a}_T\}$, the imitative expert policy $\pi^E : \mathcal{S} \rightarrow \mathcal{A}$ can be obtained by maximizing the log-likelihood over \mathcal{D}^E :

$$\pi^E := \operatorname{argmax}_{\pi} \mathbb{E}_{(\mathbf{a}, \mathbf{s}) \sim \mathcal{D}^E} [\log \pi(\mathbf{a}|\mathbf{s})]. \quad (5)$$

In a general behavioral cloning setup, the expert policy is a neural network parameterized by θ , which takes a vector of state inputs and generates a single deterministic output that represents the action, $\mathbf{a}_t = \pi_{\theta}(\mathbf{s}_t)$. Commonly, the policy network gets trained by minimizing the mean squared error (MSE) between the network outputs and expert actions, shown as

$$\mathcal{L}(\theta) = \mathbb{E}_{(\mathbf{a}, \mathbf{s}) \sim \mathcal{D}^E} \|\pi_{\theta}(\mathbf{s}) - \mathbf{a}\|^2. \quad (6)$$

A deterministic policy that outputs a point estimation of actions can be obtained through behavior cloning. To convert the point estimation to an action distribution to guide the exploration of the RL agent, we can treat the point estimation as the mean value of a Gaussian distribution and add a fixed stand deviation.

C. Aleatoric uncertainty estimation

Human (expert) behaviors are naturally stochastic, so that the deterministic policy cannot capture the uncertainty of human (expert) behaviors. This is called data uncertainty or aleatoric uncertainty [23], which originates from the potential intrinsic randomness of generating actions. To account for this kind of uncertainty, instead of outputting a deterministic action, we can take the recourse of outputting the parameters of a parametric probability distribution over actions. Assuming the action is subject to a Gaussian distribution, i.e. $\mathbf{a}_t \sim \mathcal{N}(\mu_\theta(\mathbf{s}_t), \sigma_\theta^2(\mathbf{s}_t))$, we employ the maximum likelihood estimation to train the imitative expert prior policy, which is equivalent to minimize the negative log-likelihood (NLL) function of the Gaussian distribution [24]:

$$\mathcal{L}(\theta) = \mathbb{E}_{(\mathbf{a}, \mathbf{s}) \sim \mathcal{D}^E} \left[\frac{\log \hat{\sigma}_\theta^2(\mathbf{s})}{2} + \frac{(\mathbf{a} - \hat{\mu}_\theta(\mathbf{s}))^2}{2\hat{\sigma}_\theta^2(\mathbf{s})} + c \right], \quad (7)$$

where θ is the parameters of the policy network, $\hat{\mu}_\theta$ and $\hat{\sigma}_\theta^2$ are the predictive mean and variance respectively, and c is a constant.

This way, we can obtain a stochastic policy that represents the expert's stochastic behavior.

D. Epistemic uncertainty estimation

Although we have derived a stochastic expert policy, the predictive mean and the variance of the policy are uncontrollable and unreliable, for the data that are not included in the demonstration dataset. This is called epistemic uncertainty [23], which is caused by insufficient coverage of certain areas in the state space. Estimating epistemic uncertainty is crucial for the imitative expert policy in our proposed method, because it quantifies whether the imitative policy is confident about its action outputs. Some approaches have been brought forward to estimate this kind of uncertainty, such as the Monte Carlo dropout method [25], [26] and deep ensembles method [24], [27]. In this paper, we use the deep ensembles method because it is more computationally efficient and simple to implement. We consider ensembles of M models (θ_i referring to the parameters of i -th model) trained with different random initialization using Eq. (7). The mixture mean and variance of the ensemble become:

$$\mu_{\pi^E}(\mathbf{s}) = \frac{1}{M} \sum_{i=1}^M \hat{\mu}_{\theta_i}(\mathbf{s}), \quad (8)$$

$$\sigma_{\pi^E}^2(\mathbf{s}) = \frac{1}{M} \sum_{i=1}^M \hat{\sigma}_{\theta_i}^2(\mathbf{s}) + \left[\frac{1}{M} \sum_{i=1}^M \hat{\mu}_{\theta_i}^2(\mathbf{s}) - \mu_{\pi^E}^2(\mathbf{s}) \right]. \quad (9)$$

We can now obtain a stochastic expert policy with mean $\mu_{\pi^E}(\mathbf{s})$ and variance $\sigma_{\pi^E}^2(\mathbf{s})$ that also captures the uncertainty for out-of-distribution states. Qualifying this uncertainty is helpful when the RL agent runs into states that are not included in the demonstration dataset.

IV. DEEP REINFORCEMENT LEARNING WITH IMITATIVE EXPERT PRIORS

A. Framework

Fig. 1 shows the conceptual framework of our method, which consists of three key steps: expert demonstration, policy derivation, and reinforcement learning. First and foremost, a human expert demonstrates their execution of the task, and their behaviors are encoded as sequences of state-action pairs. Then, the imitative expert policy is derived based on the demonstration data using methods from Section III. The imitative policy assumes the actions the human expert would execute in various states and it can be queried with a state by the RL agent and responds with the reference action. Finally, the imitative expert policy is applied to bias the learning process of the RL agent, by regularizing the distributional discrepancy between the agent's policy and the expert one, which is detailed below.

In the policy derivation step, we propose to add uncertainty quantification to the imitative expert policy. The intuition behind it is that when the uncertainty is small (the variance is small), meaning the policy is confident about its outputs, the RL agent's action should be close to the expert policy to avoid unnecessary exploration. In contrast, if the uncertainty is large (the variance is high), the mean value of the expert policy may not be sensible but it can admit a high variance, such that the resulting distribution may cover sensible actions. In this situation, the RL agent's action should also be close to the expert policy to explore more and find better actions.

B. Actor-critic algorithm

For the agent learning step, we use the actor-critic RL algorithm. It is a combination of policy gradients and approximate dynamic programming. Same as SAC [22], we concurrently train four networks, which are two Q-function networks (Q_{ϕ_1} and Q_{ϕ_2}), a value function network (V_ψ), and a stochastic policy network (π_θ). The Q-function networks are trained to minimize the mean-squared Bellman error (MSBE):

$$\mathcal{L}(\phi_i) = \mathbb{E}_{(\mathbf{s}_t, \mathbf{a}_t, r_t, \mathbf{s}_{t+1}) \sim \mathcal{D}} \left[\left(Q_{\phi_i}(\mathbf{s}_t, \mathbf{a}_t) - (r_t + \gamma \bar{V}_\psi(\mathbf{s}_{t+1})) \right)^2 \right], \quad (10)$$

where $i = 1, 2$, \mathcal{D} is the experience replay buffer consisting of a large number of transition tuples, and \bar{V}_ψ is the target value function, which is updated once per the main value network V_ψ update by Polyak averaging.

The value function network V_ψ gets update obeying the following equation:

$$\mathcal{L}(\psi) = \mathbb{E}_{\substack{\mathbf{s}_t \sim \mathcal{D} \\ \tilde{\mathbf{a}}_t \sim \pi_\theta(\cdot | \mathbf{s}_t)}} \left[\left(V_\psi(\mathbf{s}_t) - \min_{i=1,2} Q_{\phi_i}(\mathbf{s}_t, \tilde{\mathbf{a}}_t) \right)^2 \right], \quad (11)$$

where the actions are sampled fresh from the policy $\tilde{\mathbf{a}}_t \sim \pi_\theta(\cdot | \mathbf{s}_t)$, whereas the states should come from the replay buffer $\mathbf{s}_t \sim \mathcal{D}$.

The policy network $\pi_\theta(\cdot | \mathbf{s}_t)$ outputs the parameters of a parametric distribution, i.e. the mean and variance of a Gaussian distribution, $\mathbf{a}_t \sim \mathcal{N}(\mu_\theta(\mathbf{s}_t), \sigma_\theta^2(\mathbf{s}_t))$. The policy

network is trained to maximize the value function in each state, and thus the loss function for the policy network becomes:

$$\mathcal{L}(\theta) = \mathbb{E}_{\substack{\mathbf{s}_t \sim \mathcal{D} \\ \tilde{\mathbf{a}}_t \sim \pi_\theta(\cdot|\mathbf{s}_t)}} \left[-\min_{i=1,2} Q_{\phi_i}(\mathbf{s}_t, \tilde{\mathbf{a}}_t) \right]. \quad (12)$$

Next, we introduce two approaches to integrate the imitative expert priors into the actor-critic algorithm.

C. Expert priors as policy penalty

To encourage the learned policy to be close to the expert policy, we can add a penalty term into the reward function, leading to the refactored reward function:

$$\bar{r}(\mathbf{s}_t, \mathbf{a}_t) = r(\mathbf{s}_t, \mathbf{a}_t) - \alpha D(\pi_\theta(\cdot|\mathbf{s}_t), \pi^E(\cdot|\mathbf{s}_t)), \quad (13)$$

where α is a temperature parameter, and D is a probability metric to measure the divergence between two distributions over actions and is chosen to be the Kullback–Leibler (KL) divergence.

This is equivalent to directly incorporate the penalty term into the value function. Therefore, the update objective of the value function network (Eq. (11)) can be rewritten as

$$\mathcal{L}(\psi) = \mathbb{E}_{\substack{\mathbf{s}_t \sim \mathcal{D} \\ \tilde{\mathbf{a}}_t \sim \pi_\theta(\cdot|\mathbf{s}_t)}} \left[\left(V_\psi(\mathbf{s}_t) - \left(\min_{i=1,2} Q_{\phi_i}(\mathbf{s}_t, \tilde{\mathbf{a}}_t) - \alpha D_{KL}(\pi_\theta(\cdot|\mathbf{s}_t), \pi^E(\cdot|\mathbf{s}_t)) \right) \right)^2 \right], \quad (14)$$

where $\pi_\theta(\cdot|\mathbf{s}_t)$ is the learned policy and $\pi^E(\cdot|\mathbf{s}_t)$ is the expert policy we have obtained through imitation learning with uncertainty quantification. They are both modeled as the Gaussian distribution over actions conditioned on states.

Accordingly, the policy should maximize the refactored value function in each state, and thereby the loss function for the policy network (Eq. (12)) should be modified as:

$$\mathcal{L}(\theta) = \mathbb{E}_{\substack{\mathbf{s}_t \sim \mathcal{D} \\ \tilde{\mathbf{a}}_t \sim \pi_\theta(\cdot|\mathbf{s}_t)}} \left[-\min_{i=1,2} Q_{\phi_i}(\mathbf{s}_t, \tilde{\mathbf{a}}_t) + \alpha D_{KL}(\pi_\theta(\cdot|\mathbf{s}_t), \pi^E(\cdot|\mathbf{s}_t)) \right]. \quad (15)$$

D. Expert priors as policy constraint

Instead of adding a penalty term to the value function, we can explicitly constrain the deviation between the learned policy and expert policy within a small value. Hence, the constrained optimization problem for policy learning can be formulated as

$$\begin{aligned} \min_{\pi} \quad & \mathbb{E}_{\substack{\mathbf{s}_t \sim \mathcal{D} \\ \tilde{\mathbf{a}}_t \sim \pi_\theta(\cdot|\mathbf{s}_t)}} \left[-\min_{i=1,2} Q_{\phi_i}(\mathbf{s}_t, \tilde{\mathbf{a}}_t) \right], \\ \text{s.t.} \quad & D_{KL}(\pi_\theta(\cdot|\mathbf{s}_t), \pi^E(\cdot|\mathbf{s}_t)) \leq \epsilon, \end{aligned} \quad (16)$$

where ϵ is a small positive constant or the tolerance of the KL divergence, which represents the closeness of the learned policy to the imitative expert policy.

To solve this constrained optimization problem, we construct a corresponding Lagrangian dual problem:

$$\begin{aligned} \max_{\lambda} \min_{\pi} \quad & \mathbb{E}_{\substack{\mathbf{s}_t \sim \mathcal{D} \\ \tilde{\mathbf{a}}_t \sim \pi_\theta(\cdot|\mathbf{s}_t)}} \left[-\min_{i=1,2} Q_{\phi_i}(\mathbf{s}_t, \tilde{\mathbf{a}}_t) \right. \\ & \left. + \lambda (D_{KL}(\pi_\theta(\cdot|\mathbf{s}_t), \pi^E(\cdot|\mathbf{s}_t)) - \epsilon) \right], \end{aligned} \quad (17)$$

where λ is the non-negative Lagrangian multiplier $\lambda \geq 0$.

We can employ the dual gradient descent method to optimize the unconstrained objective by alternating gradient descent steps on θ and λ respectively [28]. The core idea is to first solve the Lagrangian function (Eq. (17)) with respect to the policy π_θ under the current Lagrangian multiplier λ (starting with a random guess), and then update the Lagrange multiplier λ if the constraint is violated. Therefore, the modified loss function for the policy network is:

$$\begin{aligned} \mathcal{L}(\theta) = \mathbb{E}_{\mathbf{s}_t \sim \mathcal{D}} \left[\mathbb{E}_{\tilde{\mathbf{a}}_t \sim \pi_\theta(\cdot|\mathbf{s}_t)} \left[-\min_{i=1,2} Q_{\phi_i}(\mathbf{s}_t, \tilde{\mathbf{a}}_t) \right. \right. \\ \left. \left. + \lambda (D_{KL}(\pi_\theta(\cdot|\mathbf{s}_t), \pi^E(\cdot|\mathbf{s}_t)) - \epsilon) \right] \right]. \end{aligned} \quad (18)$$

The Lagrangian multiplier λ gets updated according to the following loss function with the constraint $\lambda \geq 0$:

$$\mathcal{L}(\lambda) = \mathbb{E}_{\mathbf{s}_t \sim \mathcal{D}} [-\lambda (D_{KL}(\pi_\theta(\cdot|\mathbf{s}_t), \pi^E(\cdot|\mathbf{s}_t)) - \epsilon)]. \quad (19)$$

The update of the value function network remains the same as Eq. (11).

V. EXPERIMENTAL SETUP

A. Driving scenarios

We validate our proposed algorithm in solving urban autonomous driving problems. Two challenging urban driving scenarios are devised based on the SMARTS simulation platform [29]. In Fig. 2(a), the autonomous driving agent is required to complete an unprotected left turn task in heavy traffic. The agent needs to turn left onto a major road, crossing a two-way four-lane road and reaching the rightmost lane, without the regulation of traffic lights. The traffic flow is dense on the main road (each lane with a flow rate of 40 vehicles/hour). The behaviors of the environment vehicles follow the models of SUMO (car-following, lane-changing, and intersection). Fig. 2(b) shows a first-person view from the ego vehicle in the left turn scenario, which is for a human expert to observe the environment. In Fig. 2(c), a roundabout scenario is designed and the autonomous driving agent needs to safely navigate from the start point to the destination. The traffic flow rate in the roundabout is 300 vehicles/hour and the vehicles on the road are coded by a mixture of driving styles with respect to lane changing and waiting at junctions. The green areas in Fig. 2 show the accessible routes of the ego vehicle and the waypoints as far as 50 meters ahead of the ego are displayed. In each scenario, we use 20 random seeds to generate different traffic flows to simulate various situations.

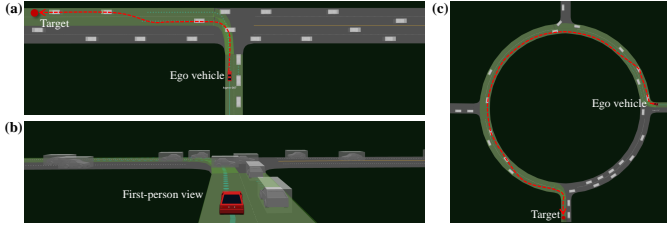


Fig. 2: The designed urban driving scenarios in the SMARTS platform: (a) unprotected left turn; (b) first-person view for expert demonstration; (c) roundabout.

B. MDP formulation

1) *Observation space*: we use a bird-eye view image encoding the environment information within a square area of 32×32 meters with the ego vehicle at the center, which is assumed to be obtained from an upstream perception module. The bird-eye view image is an RGB image of the abstracted driving scene (see Fig. 3), in which the grey area is the road, the red rectangle is the ego vehicle, and the white rectangles are the surrounding vehicles. Since such a representation encodes a rich amount of information about the road structure and interaction situations and can cope with an arbitrary number of objects, it is suitable for highly interactive urban driving scenarios. The size of the bird-eye view image is $80 \times 80 \times 3$, which means the resolution of the detection is 0.4 m/pixel.

2) *Action space*: we adopt a lane following controller that allows a high-level target input (i.e., target speed V_T and lane change L_T) to control the vehicle rather than direct vehicle control commands (e.g., steering and accelerator). The longitudinal motion control is the continuous target speed V_T within the range of $[0, 10]$ m/s, which is then normalized into $[-1, 1]$. The lateral motion is determined by the discrete lane change action L_T , namely change to the left lane $L_T = -1$, lane-keeping $L_T = 0$, and change to the right lane $L_T = +1$. To adapt the discrete action into a continuous action that can fit our proposed method, we discretize a continuous range $[-1, 1]$ into three equal-sized bins, and each bin represents a discrete action, e.g., $[-1, -1/3]$ belongs to the action of change to the left lane and $[-1/3, 1/3]$ belongs to the lane-keeping action.

3) *Reward function*: we use a sparse reward function, which only emits a meaningful value at the end of a training episode:

$$r(s, a) = r_{\text{collision}} + r_{\text{goal}}, \quad (20)$$

where $r_{\text{collision}} = -1$ is the penalty for colliding with other objects and $r_{\text{goal}} = 1$ is the reward for reaching the goal position, which are all zeros otherwise.

C. Expert demonstration

We ask a human expert to execute the designed urban driving tasks in the simulator and collect their actions as expert demonstration data. A human expert observes the driving environment in a first-person view (see Fig. 2(b)) and provides their actions, and there are four discrete actions that a human expert can manipulate through a keyboard. For the longitudinal

direction, two discrete actions, speed up (increase the speed by 2 m/s) and slow down (decrease the speed by 2 m/s), are used to set the target speed for the vehicle. For the lateral movement, two discrete actions (change to the left lane and the right lane) are used, and the default maneuver is to keep the current lane. The human expert can execute the longitudinal and lateral control actions simultaneously but need not provide actions at every timestep. The vehicle will adhere to executing the last set target until the target has been altered by the expert. We also let the expert demonstrate different behaviors in the unprotected left turn task, e.g., aggressive behavior like nudging forward in the intersection and conservative behavior like stopping to find an acceptable gap. The demonstration data is stored in the format of state-action pairs and only the successful executions of the task count. We collect 30 trajectories of the human expert demonstration in each driving scenario and behavior.

D. Comparison baselines

Some RL and IL methods are utilized as the baselines to benchmark the performance and efficiency of the proposed RL method. The baselines methods are listed as follows.

- Soft actor critic (SAC) [22]. SAC is the state-of-the-art off-policy RL algorithm, which optimizes a trade-off between the expected return and entropy. We adopt the version that can automatically tune the entropy parameter.
- Proximal policy optimization (PPO) [30] with pretrained actor network. PPO is an on-policy policy gradient RL algorithm that can stabilize the actor training by limiting the new policy not getting far from the old policy using a clipped surrogate objective function. However, this on-policy algorithm is very sample inefficient, and thus we use a pre-trained policy network instead of training from scratch.
- Generative adversarial imitation learning (GAIL) [31]. GAIL uses expert demonstration to recover a policy using generative adversarial training. The policy is the generator that gets trained with an RL algorithm using a surrogate reward given by the discriminator, which measures the similarity between generated and demonstration samples. Likewise, the policy network is also pre-trained with behavioral cloning.
- Behavioral cloning (BC). BC is a supervised learning method with the objective of reproducing the expert demonstration actions at given states (see Section III). Since the learning mechanism of BC is different from RL training, it is only compared against our method in the testing phase.

E. Implementation details

The structure of the networks are shown in Fig. 3. All the networks share the same structure of the state encoder, which consists of four convolutional layers, followed by different structures of fully connected layers for different networks to generate desired outputs. The parameters of the convolutional layers are given in the figure in a tuple format, following the meaning of (number of convolution kernels, kernel size,

and moving stride). The numbers of hidden units of the fully connected layers are also given. The action distribution, which consists of two continuous actions with respect to longitudinal and lateral motion control, is modeled as a multivariate Gaussian distribution. The policy network generates the parameters of the distribution. All the layers, if not explicitly notate in Fig. 3, use the ReLU activation function. All the networks are trained with Adam optimizer in Tensorflow using an NVIDIA RTX 2080 Super GPU.

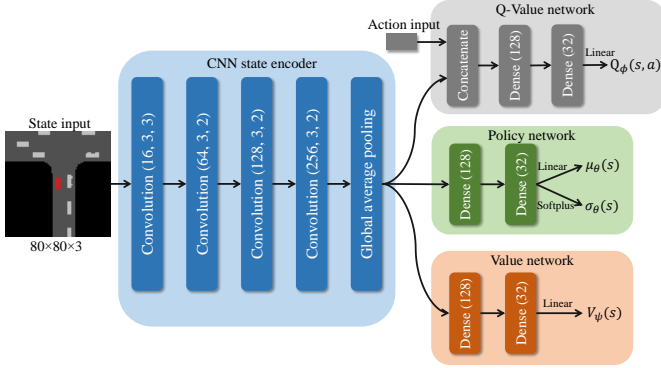


Fig. 3: The structures of the neural networks

For training the imitative expert policies, a small random number is added to the expert actions, which are discretely distributed on some specific values, so as to facilitate the training. The imitative expert policy employs the same structure, except that the output is deterministic numbers instead for the parameters of a Gaussian distribution, if using just behavioral cloning without uncertainty quantification. The expert policy network is trained for 100 epochs. For the uncertainty estimation, we train five ensemble models with different random seeds, both in the initialization of the network and shuffle of the dataset. The minimum standard deviation of the Gaussian distribution of action is restricted to 0.1, while the maximum standard deviation is unbounded.

The simulation interval is 0.1 seconds, which means the agent makes decisions every 0.1 seconds. The simulation runs on an AMD Ryzen 3900X CPU, and takes roughly one hour to finish 100,000 steps of sampling in the simulated environment. The hyperparameters used in this paper are carefully tuned to achieve the best training performance and the final settings are listed in Table I.

TABLE I: Hyperparameters used in the experiment

Symbol	Meaning	Value
M	Number of the ensemble models	5
α	KL divergence parameter	0.005
λ_0	Initial Lagrange multiplier	0.1
ϵ	KL divergence tolerance	1.0
N_B	Size of the replay buffer	20000
\mathcal{B}	Training batch size	32
lr	Learning rate	0.0003
γ	Discount rate	0.99
N_{warm}	Warm-up steps	5000
N_{train}	Total training steps	100000

VI. RESULTS AND DISCUSSIONS

A. Training results

We utilize the proposed method along with baseline methods to train an autonomous driving agent in the designed driving scenarios. In the unprotected left turn scenario, the human expert purposely demonstrates two distinct driving styles, namely conservative and aggressive. Conservative behavior is reflected by that a driver would always stop at the intersection, waiting for enough gap to cross without interrupting other vehicles, whereas aggressive behavior means that a driver would nudge forward in the intersection to show their aggressiveness, forcing other vehicles on the main road to yield. In the roundabout scenario, the goal of the human expert is to quickly pass through the roundabout and avoid collisions (efficiency and safety). Note that the expert policy here is derived with deep ensemble uncertainty estimation, and other methods will be discussed subsequently. For each method, ten trials are conducted with different random seeds to reflect the average training performance of that method. There are two correlated metrics to gauge the training performance, which are episodic reward and success rate. The episodic reward is the cumulative reward the agent gets in a training episode, and the success rate is defined as the number of successfully finished episodes over the last 20 episodes divided by 20.

Fig. 4 shows the training results of different methods in the urban driving scenarios, in which the training curve is represented by a solid line of the mean value and an error band of the 95% confidence interval. To smooth the training curve, the average episodic reward and success rate at each step are the exponentially weighted moving average over the immediate 3000 steps. In the unprotected left turn scenario, our proposed methods (both policy penalty and policy constraint methods) have achieved the best performance. Generally, the policy penalty method (adding a penalty of KL divergence to the reward function) is more favorable than the policy constraint method (constraining the KL divergence to a small tolerance). This might because the reward feedback from the environment is sparse, and adding additional feedback to the reward could help better estimate the value of actions and states. In terms of the difference in expert policies learned from different driving behaviors, we can tell that aggressive driving behavior can obtain a marginally higher success rate. One possible reason is that the environment vehicles are coded to yield to the ego vehicle if violating the safety requirement, and aggressive driving behavior may exploit this feature. In addition to the boost in training performance, our method shows a significant improvement in sample efficiency. It only takes 40% of interaction steps to reach the same performance as that of SAC (the state-of-the-art RL algorithm), improving the sample efficiency by 60%. While SAC is randomly searching for better actions, the imitative expert policy used in our method could provide a reasonable direction for searching desired actions, thus remarkably enhancing the sample efficiency. The other two baselines, PPO and GAIL with pre-trained policy network, do not perform very well. The training process of PPO is unstable, in which the performance varies significantly between different trials, and the performance is not improved

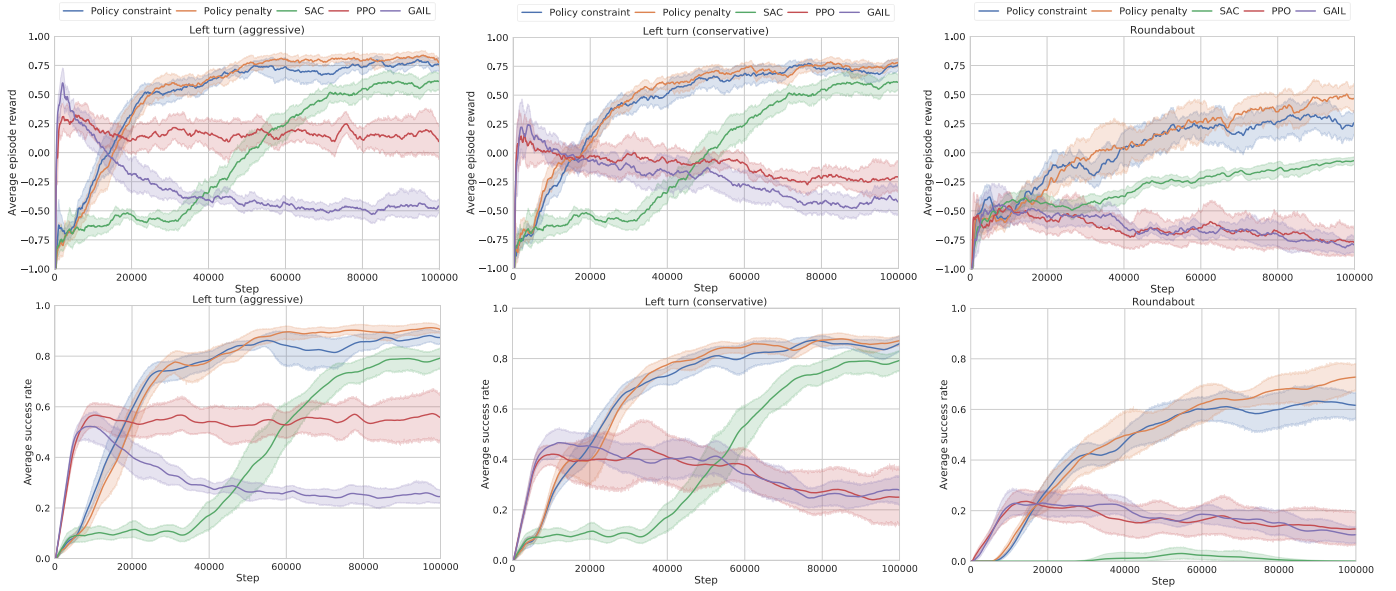


Fig. 4: The training processes of different learning methods in the urban driving scenarios: the left shows the average episodic reward and average success rate in the unprotected left turn scenario with aggressive expert policy, the middle shows those of the left turn scenario with conservative expert policy, and the right shows those of the roundabout scenario.

compared to the pre-trained policy at the beginning. The performance of GAIL, which uses a surrogate reward from the discriminator instead of the reward from the environment, collapses after several thousand steps. The performance of PPO and GAIL both degrades when using the pre-trained policy learned from conservative driving behavior.

In the roundabout scenario, our proposed method really shows its advantages, achieving a much higher success rate than other methods. Unlike the left turn scenario where difficult decisions are made in a small fragment of the scene (the intersection), the roundabout scenario is more difficult, involving more complicated situations and a longer time to finish the task. Because of the longer time horizon and sparse reward, SAC fails to estimate the values of actions and find better actions accordingly. The agent only learns to stop or creep on the road to avoid collisions with surrounding vehicles, and thereby performs the worst. PPO and GAIL act better than SAC, but likewise, the improvement comes from the pre-trained policy, and algorithms themselves can hardly improve the policy.

B. Testing results

We now begin to test the performance of the learned driving policies. We first generate 50 traffic flows that are different from the training situations and then let the driving policy with the best training performance (average success rate) control the ego vehicle to navigate from the start point to the target. The testing success rate in percentage, defined as the number of success episodes divided by the number of testing episodes, is used to measure the testing performance or generalization capability of driving policies learned from different learning methods and demonstration behaviors. The results are given in Table II.

TABLE II: Testing success rate (%) of different learning methods in the urban driving scenarios (A: aggressive, C: conservative)

	Unprotected left turn (A)	Unprotected left turn (C)	Roundabout
BC	68	80	36
GAIL	22	20	20
PPO	60	32	28
SAC	90	90	0
Ours (policy constraint)	86	92	76
Ours (policy penalty)	92	96	86

According to the data in Table II, we can conclude that the testing performance of each method is generally in line with their training performance. Our proposed policy penalty method achieves the highest testing success rate in all three situations of different driving scenarios and demonstration behaviors. The simple behavioral cloning method can outperform GAIL and PPO by a large margin, partially due to the low sample efficiency of on-policy RL algorithms. Nonetheless, our proposed method can achieve much better performance with the same number of training steps, which demonstrates higher sample efficiency. In agreement with the training results, SAC performs quite well in the unprotected left turn scenario, beating the policy constraint method with aggressive expert policy, whereas it never succeeds once in the roundabout scenario. Another finding is that the conservative behavior leads to a higher success rate, which means conservative behavior is more adaptive to the change of traffic. In addition, we list the duration of the success episode for each learning method in Table III, which clearly shows the different outcomes of driving behaviors when dealing with the unprotected left turn scenario. The duration of the driving policies with conservative driving behavior is four to five

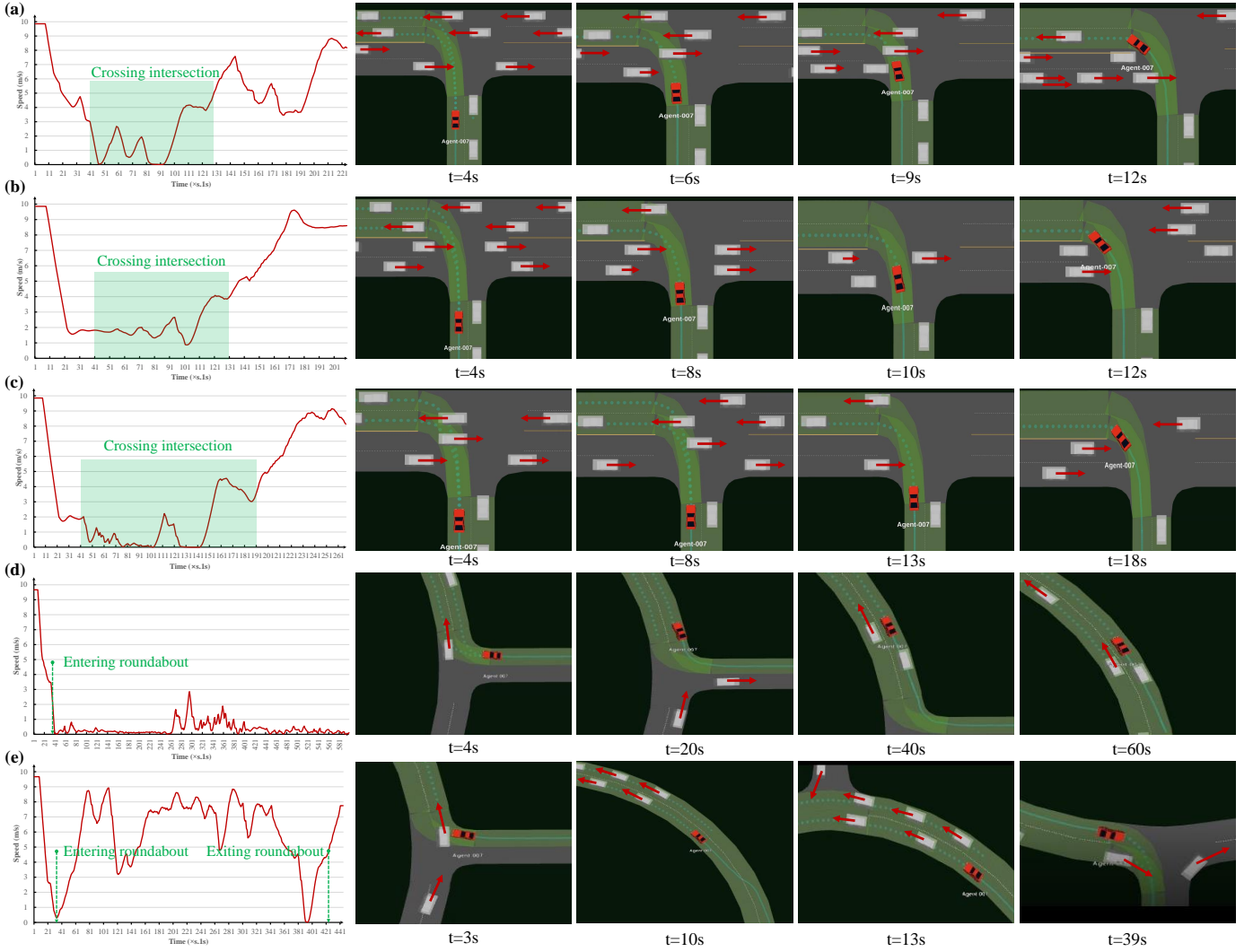


Fig. 5: Behavior analysis of different learning methods in the urban driving scenarios: (a) SAC in the unprotected left turn scenario, (b) policy penalty method with aggressive expert policy in the left turn scenario, (c) policy penalty method with conservative expert policy in the left turn scenario, (d) SAC in the roundabout scenario, (e) policy penalty method in the roundabout scenario.

seconds longer than that of aggressive behavior, because the vehicle needs to wait for enough gap in the intersection. For the SAC agent that can only access the reward of collision and reaching the target, the duration is significantly shorter than other methods, meaning its behavior is much more aggressive compared to other methods that use human expert priors in some forms. The duration of the roundabout scenario is pronouncedly longer than that of the left turn scenario, which makes SAC suffer from a long time horizon and lack of meaningful reward feedback.

As shown in Fig. 5, we analyze the behaviors of different driving policies in detail. Fig. 5(a) shows the speed curve and some representative scenes of the SAC agent in the unprotected left turn scenario. At around 4s, the ego vehicle slows down to enter the intersection and after a short pause, it goes straight into the intersection at around 6s, forcing the upcoming vehicle on the main lane to yield. Then at around 9s, the ego vehicle has to stop to avoid collision with the front

TABLE III: Testing duration (seconds) of different learning methods in the urban driving scenarios (A: aggressive, C: conservative)

	Unprotected left turn (A)	Unprotected left turn (C)	Roundabout
BC	21.49 ± 1.75	26.29 ± 2.05	42.21 ± 3.30
GAIL	23.04 ± 0.71	27.12 ± 0.42	44.30 ± 2.26
PPO	21.71 ± 1.03	26.27 ± 2.34	43.23 ± 1.45
SAC	17.88 ± 2.11	17.88 ± 2.11	—
Ours (policy constraint)	22.53 ± 1.27	25.92 ± 2.19	41.57 ± 4.63
Ours (policy penalty)	21.41 ± 0.96	25.51 ± 2.34	42.40 ± 3.54

passing vehicle while blocking one lane of the main road. After the front vehicle passes by, the ego vehicle immediately accelerates to cross, forcing the following vehicle to yield. Overall, the SAC agent is not very human-like as it would experience reckless moves like directly cut into the main road without negotiation and ignore ride comfort or smoothness. This is

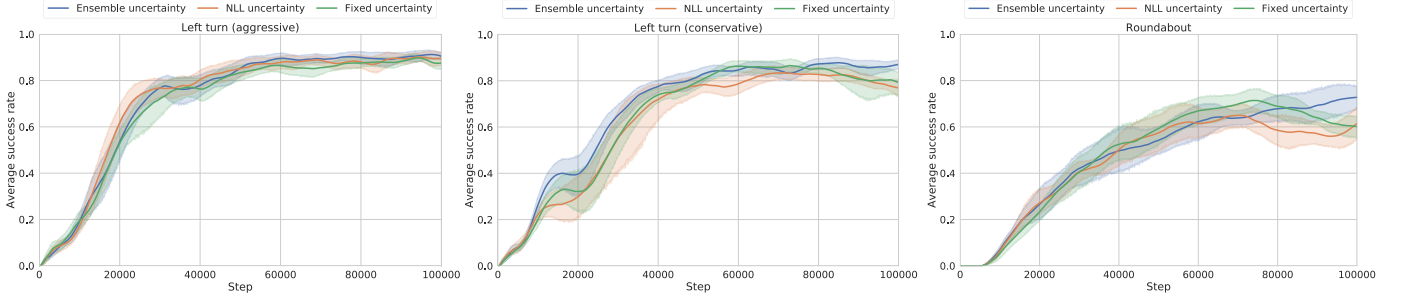


Fig. 6: The training processes of the proposed method with different expert policy derivation approaches in the urban driving scenarios: the left shows the average success rate in the unprotected left turn scenario with aggressive expert policy, the middle shows that of the left turn scenario with conservative expert policy, and the right shows that of the roundabout scenario.

mainly because it only learns to avoid collision and reach the target without the guidance of human prior knowledge. Fig. 5(b) illustrates the driving process of the policy trained by the policy penalty method with aggressive expert policy. As we can see from the speed curve and the scene at 8s, the ego vehicle keeps nudging forward in the intersection to show its aggressiveness. One human-like characteristic is reflected around 9s to 10s when the ego vehicle faces an upcoming vehicle on the main road. It first decelerates to lower the risk of collision, however, when the conflicting vehicle decelerates, the ego vehicle accelerates again to cross the intersection. For the policy penalty method with conservative expert policy, as seen in Fig. 5(c), the ego vehicle always stops at the intersection, waiting for enough clearance to cross. Another human-like characteristic is reflected around 10s to 14s when the ego vehicle nudges forward, trying to cross but a vehicle on the main lane is approaching. The ego vehicle stops again to let that vehicle pass by and then quickly accelerates to cross. In the roundabout scenario, the SAC agent, as seen in Fig. 5(d), merely creeps or even stops on the road, and thus fails to exit the roundabout. In Fig. 5(e), the agent trained with the policy penalty method has learned to stop to avoid collision when entering the roundabout (at 3s) and change to the inner lane (around 8s to 13s) to avoid interference with other vehicles at the next exit. The ego vehicle is able to stop and wait for other vehicles when exiting the roundabout (at 39s).

C. Effects of imitative expert policy

In Section III, we introduce three approaches to obtain the expert policy using imitation learning. One method is vanilla behavioral cloning that outputs a deterministic action value, and we can construct an action distribution, which is assumed to be a Gaussian, with the deterministic action as the mean value and a fixed standard deviation. The other two methods are uncertainty-aware, one of which uses the negative log-likelihood (NLL) to train a Gaussian distributional policy to capture the aleatory uncertainty, and the other uses deep ensemble to obtain a Gaussian mixture distribution to capture both the aleatory and epistemic uncertainties. The fixed uncertainty is set as the average standard deviation of the encountered states given by the deep ensemble estimation method when training, which is 0.2. We now investigate the influence of choosing different expert policy derivation methods on the

training and testing performance of our proposed method, and only the average success rate is employed as the metric. Note that the basis is the policy penalty method since it delivers better results, as seen in Fig. 4.

The results in Fig. 6 indicates that there is no significant difference between these methods in the unprotected left turn scenario, as they all can guide the RL training effectively, improving the policy to a satisfactory level. However, the expert policy with deep ensemble uncertainty estimation can lead to a marginally better performance than other methods in terms of average success rate. Besides, the expert policy with NLL-estimated uncertainty does not show a notable benefit over the fixed uncertainty method. The data in Table IV about the testing success rate of different expert policy derivation methods demonstrates that the expert policy with ensemble uncertainty estimation can also provide better testing performance, leading to better robustness and generalization ability. It is worth noting that in the roundabout scenario, the difference between these methods is more significant, and the ensemble-estimated uncertainty stands out. This is probably due to that the task of passing through the roundabout is more difficult and involves various subtle decision-makings, thus posing a more strict requirement on the expert policy. The deep ensemble method is more capable of learning the expert policy (generating expert action distributions) in terms of uncertainty estimation and providing reference actions, and thereby results in better performance in guiding the training of RL agents.

TABLE IV: Testing success rate (%) of the proposed method with different expert policy derivation approaches in the urban driving scenarios (A: aggressive, C: conservative)

	Unprotected left turn (A)	Unprotected left turn (C)	Roundabout
BC + fixed uncertainty	92	88	54
NLL uncertainty estimation	88	90	76
Ensemble uncertainty estimation	92	96	86

D. Discussions

The two biggest problems of RL fall into two categories: one is the low sample efficiency, which requires a massive amount of interactions, and the other is that the reward function is

hard to specify. Our proposed method can shed light on how to tackle the issues by introducing human prior knowledge. Specifically, we propose to distill human knowledge, in the form of human demonstration of executing a driving task, into the imitative expert policy, which is subsequently used to guide the training of RL agents. As manifested by the results given in the previous subsections, the strengths of our method are the improved sample efficiency (60% compared to the state-of-the-art RL algorithm) and ease of requirement of designing reward functions (only using sparse reward), which can hopefully facilitate the application of RL-enabled human-like autonomous driving systems. That being said, some weaknesses of the proposed method should be acknowledged. The major drawback is that we use human expert's high-level decisions as demonstration data, which does not scale to real-world scenarios when only the trajectories are available. Besides, more hyperparameters are introduced in the proposed algorithm and it is time-consuming to tune them to achieve the best performance. Therefore, future work will focus on utilizing naturalistic human driving data to learn expert policies and guide the training of RL agents. Moreover, more methods for deriving the expert policy should be explored.

VII. CONCLUSIONS

In this paper, a framework incorporating human prior knowledge and deep reinforcement learning is proposed and applied in autonomous driving scenarios. Our proposed method consists of three key steps: expert demonstration, policy derivation, and reinforcement learning. First of all, a human expert demonstrates their execution of the task potentially with their own preferences in the expert demonstration step. In the policy derivation step, the expert policy is obtained using imitation learning and uncertainty estimation using expert demonstration data. Finally, in the reinforcement learning step, we propose an actor-critic-based RL algorithm that can incorporate the imitative expert policy into RL training. Specially, two methods are proposed to regularize the KL divergence between the RL agent's policy and the imitative expert policy, namely policy penalty and policy constraint. In order to validate our method, two driving scenarios are designed, and two distinct driving behaviors are demonstrated by the human expert in the left turn scenario. The training results reveal that our method can not only achieve the best performance, but also significantly improve the sample efficiency in comparison with the baseline algorithms. When it comes to testing the learned driving policies in different traffic, the results also verify the outstanding performance of our method with the highest success rate. In the left turn scenario, some representative scenes are given to illustrate that the agent trained by our method can show different driving behaviors as the human expert, as well as some human-like features. Moreover, we find out that the policy penalty method is generally better performing in the environment with sparse reward, and using the expert policy derived with deep ensemble uncertainty estimation can lead to better performance, especially in the more difficult roundabout scenario.

REFERENCES

- [1] B. R. Kiran, I. Sobh, V. Talpaert, P. Mannion, A. A. A. Sallab, S. Yogamani, and P. Pérez, "Deep reinforcement learning for autonomous driving: A survey," *IEEE Transactions on Intelligent Transportation Systems*, pp. 1–18, 2021.
- [2] A. Haydari and Y. Yilmaz, "Deep reinforcement learning for intelligent transportation systems: A survey," *IEEE Transactions on Intelligent Transportation Systems*, pp. 1–22, 2020.
- [3] Z. Huang, J. Wu, and C. Lv, "Driving behavior modeling using naturalistic human driving data with inverse reinforcement learning," *IEEE Transactions on Intelligent Transportation Systems*, pp. 1–13, 2021.
- [4] S. Rosbach, V. James, S. Großjohann, S. Homoceanu, and S. Roth, "Driving with style: Inverse reinforcement learning in general-purpose planning for automated driving," in *2019 IEEE/RSJ International Conference on Intelligent Robots and Systems (IROS)*. IEEE, 2019, pp. 2658–2665.
- [5] J. Hawke, R. Shen, C. Gurau, S. Sharma, D. Reda, N. Nikolov, P. Mazur, S. Micklethwaite, N. Griffiths, A. Shah, *et al.*, "Urban driving with conditional imitation learning," in *2020 IEEE International Conference on Robotics and Automation (ICRA)*. IEEE, 2020, pp. 251–257.
- [6] Z. Huang, C. Lv, Y. Xing, and J. Wu, "Multi-modal sensor fusion-based deep neural network for end-to-end autonomous driving with scene understanding," *IEEE Sensors Journal*, vol. 21, no. 10, pp. 11 781–11 790, 2021.
- [7] M. Bansal, A. Krizhevsky, and A. Ogale, "Chauffeurnet: Learning to drive by imitating the best and synthesizing the worst," in *Proceedings of Robotics: Science and Systems*, Freiburg/Breisgau, Germany, June 2019.
- [8] J. Chen, S. E. Li, and M. Tomizuka, "Interpretable end-to-end urban autonomous driving with latent deep reinforcement learning," *IEEE Transactions on Intelligent Transportation Systems*, 2021.
- [9] P. Palanisamy, "Multi-agent connected autonomous driving using deep reinforcement learning," in *2020 International Joint Conference on Neural Networks (IJCNN)*. IEEE, 2020, pp. 1–7.
- [10] Z. Cao, E. Biyik, W. Wang, A. Raventos, A. Gaidon, G. Rosman, and D. Sadigh, "Reinforcement learning based control of imitative policies for near-accident driving," in *Robotics: Science and Systems*, 2020.
- [11] D. Chen, L. Jiang, Y. Wang, and Z. Li, "Autonomous driving using safe reinforcement learning by incorporating a regret-based human lane-changing decision model," in *2020 American Control Conference (ACC)*. IEEE, 2020, pp. 4355–4361.
- [12] H. Krasowski, X. Wang, and M. Althoff, "Safe reinforcement learning for autonomous lane changing using set-based prediction," in *2020 IEEE International Conference on Intelligent Transportation Systems (ITSC)*, 2020.
- [13] J. Duan, S. E. Li, Y. Guan, Q. Sun, and B. Cheng, "Hierarchical reinforcement learning for self-driving decision-making without reliance on labelled driving data," *IET Intelligent Transport Systems*, vol. 14, no. 5, pp. 297–305, 2020.
- [14] J. Wu, Z. Huang, C. Huang, Z. Hu, P. Hang, Y. Xing, and C. Lv, "Human-in-the-loop deep reinforcement learning with application to autonomous driving," *arXiv preprint arXiv:2104.07246*, 2021.
- [15] X. Liang, T. Wang, L. Yang, and E. Xing, "Cirl: Controllable imitative reinforcement learning for vision-based self-driving," in *Proceedings of the European Conference on Computer Vision (ECCV)*, 2018, pp. 584–599.
- [16] M. Pfeiffer, S. Shukla, M. Turchetta, C. Cadena, A. Krause, R. Siegwart, and J. Nieto, "Reinforced imitation: Sample efficient deep reinforcement learning for mapless navigation by leveraging prior demonstrations," *IEEE Robotics and Automation Letters*, vol. 3, no. 4, pp. 4423–4430, 2018.
- [17] T. Haarnoja, A. Zhou, P. Abbeel, and S. Levine, "Soft actor-critic: Off-policy maximum entropy deep reinforcement learning with a stochastic actor," in *International Conference on Machine Learning*, 2018, pp. 1861–1870.
- [18] M. Vecerik, T. Hester, J. Scholz, F. Wang, O. Pietquin, B. Piot, N. Heess, T. Rothörl, T. Lampe, and M. Riedmiller, "Leveraging demonstrations for deep reinforcement learning on robotics problems with sparse rewards," *arXiv preprint arXiv:1707.08817*, 2017.
- [19] T. Hester, M. Vecerik, O. Pietquin, M. Lanctot, T. Schaul, B. Piot, D. Horgan, J. Quan, A. Sendonaris, I. Osband, *et al.*, "Deep Q-learning from demonstrations," in *AAAI*, 2018, pp. 3223–3230.
- [20] H. Liu, Z. Huang, and C. Lv, "Improved deep reinforcement learning with expert demonstrations for urban autonomous driving," *arXiv preprint arXiv:2102.09243*, 2021.

- [21] S. Levine, A. Kumar, G. Tucker, and J. Fu, “Offline reinforcement learning: Tutorial, review, and perspectives on open problems,” *arXiv preprint arXiv:2005.01643*, 2020.
- [22] T. Haarnoja, A. Zhou, K. Hartikainen, G. Tucker, S. Ha, J. Tan, V. Kumar, H. Zhu, A. Gupta, P. Abbeel, *et al.*, “Soft actor-critic algorithms and applications,” *arXiv preprint arXiv:1812.05905*, 2018.
- [23] E. Hüllermeier and W. Waegeman, “Aleatoric and epistemic uncertainty in machine learning: An introduction to concepts and methods,” *Machine Learning*, pp. 1–50, 2021.
- [24] B. Lakshminarayanan, A. Pritzel, and C. Blundell, “Simple and scalable predictive uncertainty estimation using deep ensembles,” in *Advances in neural information processing systems*, 2017, pp. 6402–6413.
- [25] Y. Gal and Z. Ghahramani, “Dropout as a bayesian approximation: Representing model uncertainty in deep learning,” in *international conference on machine learning*, 2016, pp. 1050–1059.
- [26] R. Michelmores, M. Wicker, L. Laurenti, L. Cardelli, Y. Gal, and M. Kwiatkowska, “Uncertainty quantification with statistical guarantees in end-to-end autonomous driving control,” in *2020 IEEE International Conference on Robotics and Automation (ICRA)*. IEEE, 2020, pp. 7344–7350.
- [27] P. Tigas, A. Filos, R. McAllister, N. Rhinehart, S. Levine, and Y. Gal, “Robust imitative planning: Planning from demonstrations under uncertainty,” in *Machine Learning for Autonomous Driving Workshop at the 33rd Conference on Neural Information Processing Systems*, 2019.
- [28] N. Siegel, J. T. Springenberg, F. Berkenkamp, A. Abdolmaleki, M. Neunert, T. Lampe, R. Hafner, N. Heess, and M. Riedmiller, “Keep doing what worked: Behavior modelling priors for offline reinforcement learning,” in *International Conference on Learning Representations*, 2020.
- [29] M. Zhou, J. Luo, J. Villela, Y. Yang, D. Rusu, J. Miao, W. Zhang, M. Alban, I. Fadarar, Z. Chen, *et al.*, “Smarts: Scalable multi-agent reinforcement learning training school for autonomous driving,” in *Conference on Robot Learning*, 2020.
- [30] J. Schulman, F. Wolski, P. Dhariwal, A. Radford, and O. Klimov, “Proximal policy optimization algorithms,” *arXiv preprint arXiv:1707.06347*, 2017.
- [31] J. Ho and S. Ermon, “Generative adversarial imitation learning,” in *Advances in neural information processing systems*, 2016, pp. 4565–4573.